ANALYSIS OF NOTCH EFFECT IN SHORT GLASS FIBRE REINFORCED POLYAMIDE 6

F.T. Ibáñez-Gutiérrez[1], S. Cicero[1] and I.A. Carrascal[1]

[1] LADICIM (Laboratory of Materials Science and Engineering), University of Cantabria, E.T.S. de Ingenieros de Caminos, Canales y Puertos, Av/ Los Castros 44, 39005, Santander, Cantabria, Spain
Email: ibanezft@unican.es, Web Page: http://www.ladicim.unican.es

Keywords: Fracture Toughness, Polyamide 6, Notch Effect

Abstract
This paper presents the analysis of the notch effect in short glass fibre reinforced polyamide 6 (SGFR-PA6) fracture specimens. The research is based on the results obtained in an experimental programme composed of 50 fracture specimens, combining two fibre contents (10 and 30 wt. %) and 5 different notch radii varying from 0 mm (crack-like defects) up to 2 mm. The notch effect is analysed through the evolution of the apparent fracture toughness and the application of the Theory of the Critical Distances. The results show a clear notch effect.
The research is completed with the analysis of the evolution of fracture micromechanisms when the radius increases by using Scanning Electron Microscopy (SEM) fractographies. It has been revealed a direct relation between this evolution and the apparent fracture toughness observations.

1. Introduction

The defects on structural components can appear in any stage of the component's life. Nevertheless, they are not necessarily sharp. Notched components present a fracture resistance (named apparent fracture toughness) which is greater than the fracture toughness observed in cracked components (e.g., [1-9]). Therefore, if notches are considered as cracks when performing fracture assessments, the corresponding results may be overconservative, increasing the costs due to premature replacements and repairs, or oversizing the structures.

In recent years, different researchs have developed a notch theory capable of predicting the fracture behaviour of notched components, proposing two main failure criteria: the global criterion and the local criteria [1,2]. The local criteria are easier to apply in practical terms and are based on the stress-strain field at the notch tip. The most important are the Point Method (PM) and the Line Method (LM), both of them belonging to the Theory of Critical Distances (TCDs). The TCD is essentially a group of methodologies, all of them using a characteristic material length parameter (the critical distance, *L*) when performing fracture assessments [10-13]. The expression in fracture analysis for the critical distance, L, follows the equation:

$$L = \frac{1}{\pi}\left(\frac{K_{IC}}{\sigma_0}\right)^2 \quad (1)$$

where K_{IC} is the material fracture toughness obtained for cracked specimens, and σ_0 is a characteristic material strength parameter (the inherent strength), usually larger than the ultimate tensile strength (σ_U), that requires calibration. Only in those situations where there is a linear-elastic behaviour at both the micro and the macro scales (e.g., fracture of ceramics) σ_0 coincides with σ_U. In fatigue analysis, L has an analogous expression that may be consulted in the bibliography [10].

Excerpt from ISBN 978-3-00-053387-7

Among the different methodologies mentioned of the TCD, the PM and the LM are particularly simple to apply. The PM states that fracture occurs when the stress reaches the inherent strength (σ_0) at a distance ($L/2$) from the defect tip [10,14]. The LM, meanwhile, assumes that fracture occurs when the average stress along a distance from the defect tip, $2L$, reaches the inherent strength (σ_0). Eqs. (2) and (3), respetively, summarise both approaches:

$$\sigma\left(\frac{L}{2}\right) = \sigma_0 \tag{2}$$

$$\frac{1}{2L}\int_0^{2L} \sigma(r)dr = \sigma_0 \tag{3}$$

The TCD allows the fracture assessment of components with any kind of stress riser to be performed. As an example, when using the PM, it would be sufficient to perform two fracture tests on two specimens with different types of defects (e.g., sharp notch and blunt notch). The corresponding stress-distance curves at fracture, which can be determined by using analytical solutions or finite element methods, cross each other at a point with coordinates ($L/2$, σ_0), as shown in Figure 1, provided both are sufficiently sharp. The prediction of the fracture load of any other component made of the same material and containing any other kind of defect would require the definition of the corresponding stress field, the fracture load being that one for which Eq. (2) is fulfilled.

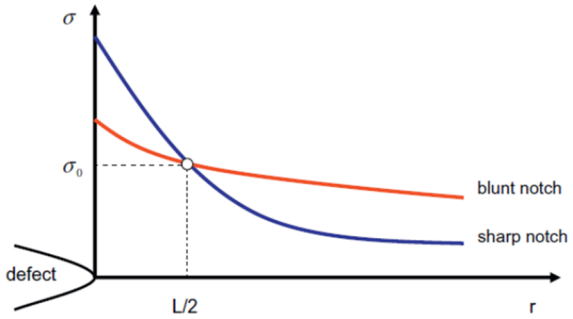

Figure 1. Obtaining L and σ_0 parameters.

Both the PM and the LM provide expressions, based on the Creager and Paris [6] notch tip stress distribution, for the apparent fracture toughness (K_{IN}) exhibited by notched components. This parameter reduces the fracture analysis in a component having a U-shaped notch to an equivalent situation in a cracked component, with the only particularity of considering K_{IN} instead of K_{IC}. The expressions derived from the PM and the LM are, respectively (ρ is the notch radius):

$$K_{IN} = K_{IC}\frac{\left(1+\frac{\rho}{L}\right)^{\frac{3}{2}}}{\left(1+\frac{2\rho}{L}\right)} \tag{4}$$

$$K_{IN} = K_{IC}\sqrt{1+\frac{\rho}{4L}} \tag{5}$$

Finally, the TDC is known and used to predict failure in composite materials [10]. However, the PM and the LM have been only used to predict the fracture strength of many kinds of composites. The aim of this research is, on the one hand, to study the notch effect in the apparent fracture toughness; and, on the other hand, to analyse the evolution of fracture micromechanisms when the radius increases.

Excerpt from ISBN 978-3-00-053387-7

2. Experimental programme

2.1. Material

The material chosen for this research is short glass fibre reinforced polyamide 6 (SGFR-PA6). Short fibre reinforced thermoplastics (SFRTs) constitute an important class of technical plastics which are replacing metal parts in engineering components due to their easy fabrication and good mechanical properties [15]. The monomer of PA 6 is one of the most common commercial grades for moulded parts, leading to high strength, high stiffness, good toughness, translucency, good fatigue life and good abrasion resistance [16]. Reinforcing PAs with short glass fibres leads to a significant increase in strength, stiffness, heat distortion temperature and abrasion resistance. In the last decades, as a consequence of these favourable properties, SGFR-PA 6 has found an increasing number of applications in the automotive and railway industries. Such applications imply the existence of notches or stress risers on the component that may put at risk its structural integrity. To perform a comparative study, two different amounts of fibre content have been selected for the present research: 10 wt.% and 30 wt.%.

2.2. Methodology and results

In order to analyse the notch effect on the apparent fracture toughness SGFR-PA6, the TDC has been used. The TDC parameters have been calibrated with fracture tests on notched specimens. A total amount of 54 tensile specimens were obtained by means of injection moulding in previously fabricated moulds, with the fibres oriented in the longitudinal direction of the specimen. Table 1 gathers the main characteristics of the glass fiber used. The geometry of the tensile specimens is shown in Figure 2a.

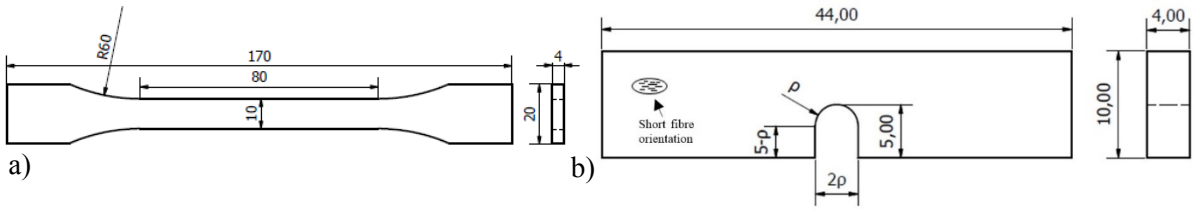

Figure 2. a) Tensile specimens (mm); **b)** SENB test specimen (mm); ρ varying from 0 mm to 2 mm.

Table 1. E-glass fibre parameters.
L: length; Ø: diameter; σ_U: ultimate tensile strength; E: Elastic Modulus; ρ: density.

L (μm)	Ø (μm)	σ_U (MPa)	E (GPa)	ρ (g/cm^3)
300	10	3450	72.50	2.60

Firstly, two tensile tests were perfomed for each fibre content following ASTM D638 [17] at room temperature (20ºC) under displacement control conditions with a universal servo hydraulic INSTRON machine. The results obtained are shown in Table 2. It can be stated that the higher the fibre content, the larger the tensile parameters values.

Secondly, 50 Single-Edge Notch Bend (SENB) specimens were tested as per ASTM D5045 [18]. The specimens (Figure 2b) were obtained from the central part of the corresponding fabricated tensile samples. The notches were machined, except for crack-like defects (0 mm of notch radius), which were generated by sawing a razor blade [18]. 5 tests were performed per combination of fibre content (10 wt.% and 30 wt.%) and notch radius (varying from 0 mm up to 2.0 mm).

Excerpt from ISBN 978-3-00-053387-7

Table 2. Tensile parameters.
E: Elastic Modulus; $\sigma_{0.2}$: Yield Stress; σ_U: ultimate tensile strength; e_{max}: strain under maximum load.

Fibre content (%)	Test	E (GPa)	$\sigma_{0.2}$ (MPa)	σ_U (MPa)	e_{max} (%)
10	1	3.60	70.7	80.8	3.02
	2	3.50	69.6	75.5	2.65
30	1	6.40	105.5	128.4	3.55
	2	6.50	105.2	127.6	3.57

Tables 3 gathers the experimental results obtained in terms of the maximum load reached and the corresponding apparent fracture toughness (K_{IN}) which is obtained by the application of cracked specimen formulation [18] to notched specimens (Eq. 6). Only one test was invalid (30 wt.%; 0.5mm).

$$K_{IN} = \left(\frac{P_{max}}{B \cdot W^{1/2}}\right) 6 \left(\frac{a}{W}\right)^{1/2} \left(\frac{1.99 - \left(\frac{a}{W}\right)\left(1 - \frac{a}{W}\right)\left(2.15 - 3.93\left(\frac{a}{W}\right) + 2\left(\frac{a}{W}\right)^2\right)}{\left(1 + 2\left(\frac{a}{W}\right)\right)\left(1 - \frac{a}{W}\right)^{3/2}} \right) \quad (6)$$

where *Pmax* is the corresponding maximum load, *B* is the specimen thickness, *W* is the specimen width, and *a* is the defect length.

Table 3. Experimental results.

Notch radius ρ (mm)	10 wt.%			30 wt.%		
	Notch length a (mm)	Max. Load (N)	K_{IN} (MPa·m$^{1/2}$)	Notch length a (mm)	Max. Load (N)	K_{IN} (MPa·m$^{1/2}$)
0.00	4.20	117.50	2.46	4.48	253.50	5.76
0.00	4.25	107.20	2.28	4.70	195.50	4.74
0.00	4.60	70.20	1.65	4.80	195.70	4.90
0.00	4.60	76.70	1.81	4.57	171.70	4.01
0.00	4.90	95.90	2.47	4.75	180.10	4.44
0.25	5.00	93.10	2.48	5.00	237.80	6.33
0.25	5.00	105.20	2.80	5.00	220.20	5.86
0.25	5.00	104.50	2.78	5.00	202.50	5.39
0.25	5.00	87.80	2.34	5.00	216.40	5.76
0.25	5.00	78.60	2.09	5.00	205.40	5.47
0.5	5.00	116.20	3.09	5.00	207.10	5.51
0.5	5.00	102.10	2.72	5.00	252.40	6.72
0.5	5.00	93.40	2.49	5.00	251.80	6.70
0.5	5.00	111.10	2.96	-	-	-
0.5	5.00	97.70	2.60	5.00	243.30	6.48
1.00	5.00	124.10	3.30	5.00	231.60	6.17
1.00	5.00	116.50	3.10	5.00	251.50	6.70
1.00	5.00	141.00	3.75	5.00	287.90	7.67
1.00	5.00	125.00	3.33	5.00	302.60	8.06
1.00	5.00	119.70	3.19	5.00	246.60	6.57
2.00	5.00	173.80	4.63	5.00	305.80	8.14
2.00	5.00	166.70	4.44	5.00	284.20	7.57
2.00	5.00	167.30	4.45	5.00	269.00	7.16
2.00	5.00	146.40	3.90	5.00	263.70	7.02
2.00	5.00	153.40	4.08	5.00	318.30	8.47

Excerpt from ISBN 978-3-00-053387-7

Figure 3 shows the load-displacement curves obtained in some of the tests. It can be observed a clear domintant linear-elastic behaviour in all cases, although there is some non-linearity in the specimens with higher notch radii.

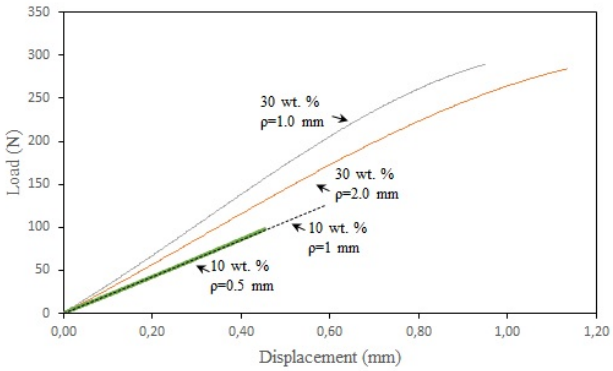

Figure 3. Load-displacement curve of some specimens.

3. Evolution of the fracture resistance

This analysis evaluates the effects of the fibre content and the notch radius on the fracture resistance. Figure 4 presents the different experimental results, the corresponding best fit curve following Eq. (5), and the LM prediction obtained using Eq. (5) with the inherent strength being equal to the ultimate tensile strength ($\sigma_0=\sigma_U$). The best fit curves have used L as the fitting parameter, and have been obtained by the least squares method and obliging the curve to take the average value of the fracture toughness (K_{IC}) obtained in the cracked specimens at $\rho=0$.

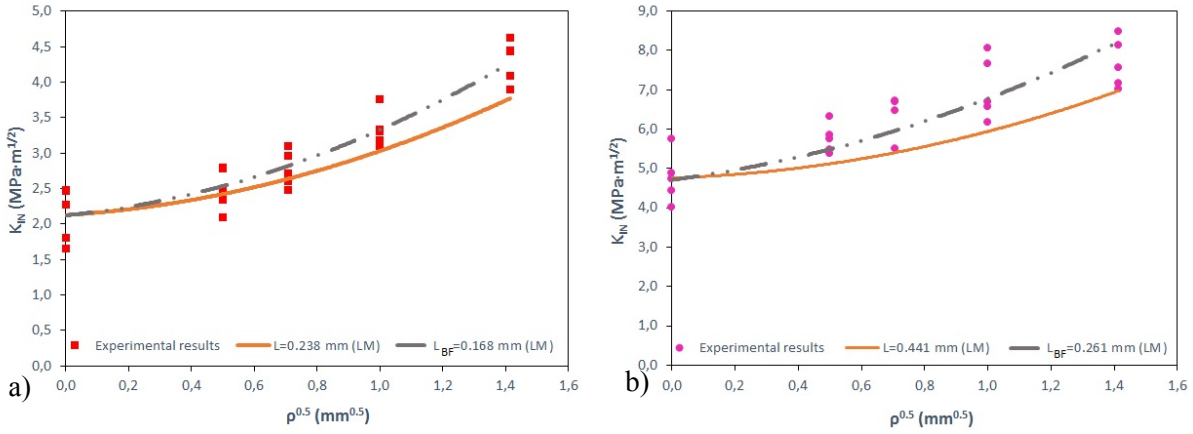

Figure 4. Evolution of the apparent fracture toughness and predictions provided by the Line Method: a) 10 wt. %; b) 30 wt. %
L: critical distance from Eq.(1) and $\sigma_0=\sigma_U$; L_{BF}: critical distance providing the best fit.

Table 4 compares the parameters associated to the different predictions. σ_U is the average of the corresponding ultimate tensile strength results obtained for each fibre content (see Table 2), L is the value of critical distance obtained from Eq. (1) and considering that σ_0 is equal to σ_U, L_{BF} is the value of the critical distance providing the best fit (least squares) to the experimental results, as mentioned above,

Excerpt from ISBN 978-3-00-053387-7

and $\sigma_{0,BF}$ is the resulting inherent strength from L_{BF} and Eq. (1). K_{IC} is the average value obtained in crack specimens.

Table 4. Material parameters (TDC).

Fibre content (%)	K_{IC} (MPa·m$^{1/2}$)	σ_U (MPa)	L (mm)	σ_0 (MPa)	L_{BF} (mm)
10	2.13	78.15	0.238	93.01	0.168
30	4.77	128.00	0.441	166.38	0.261

It is observed that L and L_{BF} provide reasonable similar predictions of the evolution of apparent fracture toughness. L provides moderately more conservative estimations, so the assumption of the inherent strength being equal to σ_U is reasonably safe for SGFR-PA6. This has important practical consequences, given that the application of the TCD to this type of materials would not require any previous calibration, with L depending directly on K_{IC} and σ_U.

In addition, the notch effect is clearly visible for both fibre contents, given that it is observed an evident increase in K_{IN} when the notch radius increases. The notch effect is larger for a low fibre content (10 wt.%).

4. Evolution of the fracture micromechanisms

The fracture micromechanisms analysis was carried out by using Scanning Electron Microscopy (SEM). The specimens observed correspond to tests providing intermediate values of apparent fracture toughness.

Figure 5 presents the fracture surfaces of specimens with a fibre content of 10 wt. %, and notch radii from 0 mm up to 2.0 mm. It can be stated that fracture micromechanisms present an evolution, with a rougher surface and more ductile aspect when the notch radius increases.

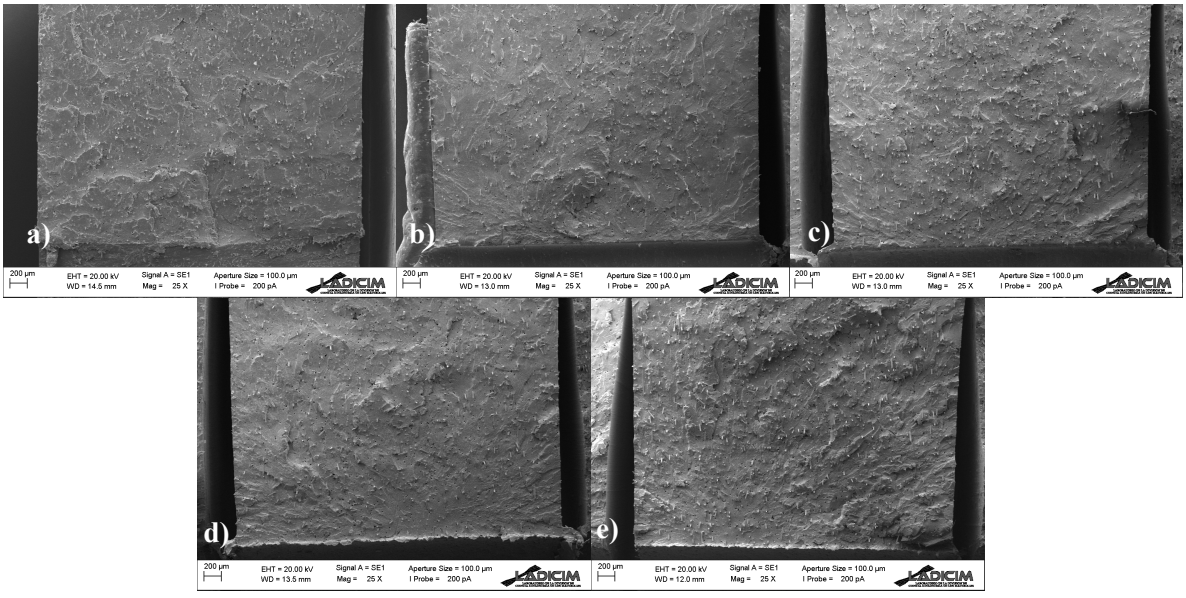

Figure 5. Evolution of the fracture micromechanisms in SGFR-PA6 10wt.%:
a) ρ = 0 mm; b) ρ = 0.25 mm; c) ρ = 0.5 mm; d) ρ = 1.0 mm; e) ρ = 2.0 mm.

Excerpt from ISBN 978-3-00-053387-7

In addition, Figure 6 presents the two fibre contents studied and two different notch radii: 0.5 mm and 2 mm. It has been observed a rougher and more non-linear aspect when the fibre content increases. This observation is in accordance with the trend of K_{IN} seen in Fig. 4 (the higher the fibre content, the higher the apparent fracture toughness). Figure 6c shows that for low fibre content the matrix material around the fibres has little deformation. However, in Figure 6d it can be observed that for high fibre contents, the matrix material around the fibres is highly strained, with a high development of non-linear micromechanisms.

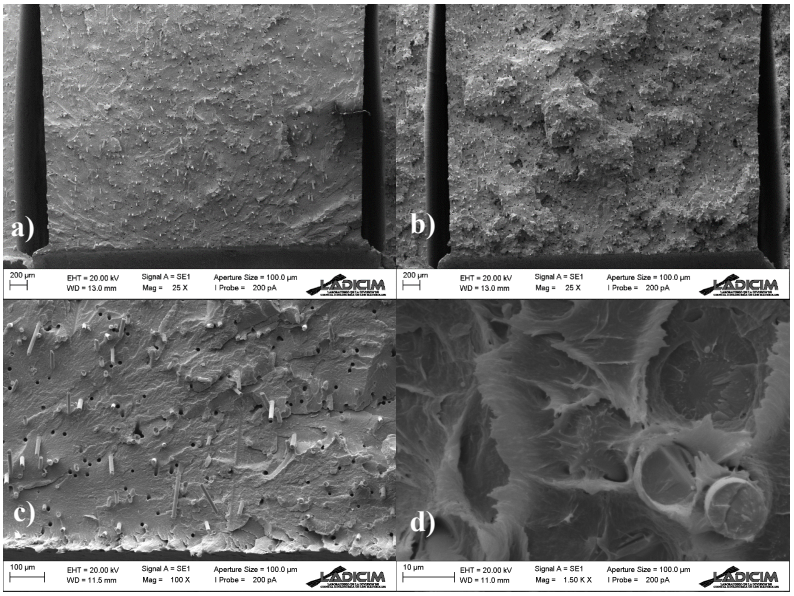

Figure 6. Detail of fracture micromechanisms:
a) 10 wt.% ρ = 0.5 mm; b) 30 wt.% ρ = 0.5 mm ; c) 10 wt.% ρ = 2 mm; d) 30 wt.% ρ = 2 mm

5. Conclusions

This paper applies and validates the Theory of Critical Distances in SGFR-PA6. The methodology has been applied to 50 SENB specimens combining two different fibre contents (10 wt.% and 30 wt.%) and five different notch radii, from 0 mm (crack-like defects) up to 2 mm.

It has been observed an evident notch effect, with an increase in the fracture resistance in notched conditions when the notch radius increases. Such notch effect has been reasonably (and conservatively) predicted by the direct application of the Line Method considering that the material inherent strength is equal to the ultimate tensile strength. This is especially significant, given that the application of this methodology to this type of materials generates straightforward and safe predicitons. Analogously, it has also been observed that the fibre content has an evident effect on the fracture resistance., given that this parameter increases when the fibre content increases.

Lastly, the SEM observation of the fracture surfaces has related the evolution of the apparent fracture toughness with the evolution of the fracture micromechanisms.

Excerpt from ISBN 978-3-00-053387-7

Acknowledgments

The authors of this work would like to express their gratitude to the Spanish Ministry of Science and Innovation for the financial support of the Project MAT2014-58443-P: "Análisis del comportamiento en fractura de componentes estructurales con defectos en condiciones debajo confinamiento tensional", on the results of which this paper is based.

References

[1] AA Griffith, The phenomena of rupture and flow in solids, Phil. Trans. R Soc. London. A 221, pp. 163-198, 1920.
[2] LS Niu, C. Chehimi, G. Pluvinage, Stress field near a large blunted V notch and application of the concept of notch stress intensity factor to the fracture of very brittle materials, Eng Fract Mech 1949;49:325-35.
[3] G. Pluvinage, Fatigue and fracture emanating from notch; the use of the notch stress intensity factor, Nucl Eng Des 1998;185:173-84.
[4] Y. Bao, Z. Jin, Size effects and mean strength criterion for ceramics, Fat Fract Eng Mater Str 1993;16:829-35.
[5] W. Fenghui, Prediction of intrinsic fracture toughness for brittle materials from the apparent toughness of notch-crack specimen, J Mater Sci 2000;35:2543.
[6] M. Creager, C. Paris, Elastic field equations for blunt cracks with reference to stress corrosion cracking, Int J Fract 1967;3:247-52.
[7] S. Cicero, F. Gutiérrez-Solana, JA. Álvarez, Structural Integrity assessment of components subjected to low constraint conditions, Eng Fract Mech 2008;35:2543-6.
[8] S. Cicero, V. Madrazo, IA. Carrascal, On the point method and the line method notch effect predictions in Al7075-T651, Eng Fract Mech 2012;86:56-72.
[9] S. Cicero, V. Madrazo, T. García, Analysis of the notch effect in the apparent fracture toughness and the fracture micromechanisms of ferritic-pearlitic steels operating within their lower shelf, Eng Fail Ana 2014;36:322-342.
[10] D. Taylor, The theory of critical distances: a new perspective in fracture mechanics, Elservier, 2007.
[11] D. Taylor, M. Merlo, R. Pegley, MP. Cavatorta, The effect of stress concentrations on the fracture strength of polymethylmethacrylate, Mater Sci Eng 2004;A382: 288–94.
[12] H. Neuber, Theory of notch stresses: principles for exact calculation of strength with reference to structural form and material, Springer Verlag, Berlin, 1958.
[13] RE. Peterson, Notch sensitivity. In: Sines G, Waisman JL, editors. Metal fatigue. McGraw Hill. 1959. p. 293–306. New York.
[14] TL. Anderson, Fracture mechanics: fundamentals and applications, CRC Press, Florida, 1991.
[15] PK. Mallik, Fibre reinforced composites; materials manufacturing and design, 3rd Edition, CRC Press, 2007.
[16] JA. Brydson, Plastics Materials, 5th Edition, Guildford: Butterworth Heinemann, 1989.
[17] ASTM D638-10, Standard Test Method for Tensile Properties of Plastics, American Society of Testing and Materials, Philadelphia, 2010.
[18] ASTM D5045-99, Standard Test Methods for Plane-Strain Fracture Toughness and Strain Energy Release Rate of Plastic Materials, American Society of Testing and Materials, Philadelphia, 1999.

Excerpt from ISBN 978-3-00-053387-7